PHILOSOPHICAL TRANSACTIONS OF THE ROYAL SOCIETY B

Phil. Trans. R. Soc. B (2012) **367**, 1525–1533
doi:10.1098/rstb.2011.0239

Research

Phloem-associated auxin response maxima determine radial positioning of lateral roots in maize

Leentje Jansen[1,2], Ianto Roberts[1,2], Riet De Rycke[1,2] and Tom Beeckman[1,2,*]

[1]*Department of Plant Systems Biology, Integrative Plant Biology Division, VIB, Technologiepark 927, 9052 Ghent, Belgium*
[2]*Department Plant Biotechnology and Bioinformatics, Ghent University, Technologiepark 927, 9052 Ghent, Belgium*

In *Arabidopsis thaliana*, lateral-root-forming competence of pericycle cells is associated with their position at the xylem poles and depends on the establishment of protoxylem-localized auxin response maxima. In maize, our histological analyses revealed an interruption of the pericycle at the xylem poles, and confirmed the earlier reported proto-phloem-specific lateral root initiation. Phloem-pole pericycle cells were larger and had thinner cell walls compared with the other pericycle cells, highlighting the heterogeneous character of the maize root pericycle. A maize DR5::RFP marker line demonstrated the presence of auxin response maxima in differentiating xylem cells at the root tip and in cells surrounding the proto-phloem vessels. Chemical inhibition of auxin transport indicated that the establishment of the phloem-localized auxin response maxima is crucial for lateral root formation in maize, because in their absence, random divisions of pericycle and endodermis cells occurred, not resulting in organogenesis. These data hint at an evolutionarily conserved mechanism, in which the establishment of vascular auxin response maxima is required to trigger cells in the flanking outer tissue layer for lateral root initiation. It further indicates that lateral root initiation is not dependent on cellular specification or differentiation of the type of vascular tissue.

Keywords: lateral root development; maize; auxin; pericycle

1. INTRODUCTION

Plant roots have a typical anatomy composed of different concentric tissues (the epidermis, cortex and the endodermis) surrounding a central vascular cylinder. The outer layer of the central cylinder is the pericycle, which is generally considered as another concentric layer, while the rest of the central tissue is radially, rather than concentrically, organized. In the model plant *Arabidopsis thaliana*, each of the outer tissues is composed of one layer, with a relatively constant number of cells. Further, the vasculature has diarch symmetry, consisting of two alternating xylem and phloem poles, and is delimited by a single layer of pericycle cells [1]. This pericycle forms the basis for the formation of lateral roots, which allow plants to adjust to their environment in a dynamic way and to overcome unequal distribution of water and nutrients in the soil [2,3].

Only a subset of the pericycle cells has the capacity to divide and to form lateral roots. In *Arabidopsis*, these cells are located at the xylem poles [4]. However, also the presence of quiescent phloem-pole pericycle cells seems to be indispensable for correct lateral root development, as *wol* mutants, completely lacking phloem, were unable to develop organized lateral root primordia [5]. In addition, several studies in various dicotyledonous species report on differing morphological, genetic and cell cycle-related properties between the xylem- and phloem-pole pericycle cells (overviews in [6,7]), suggesting the pericycle cell layer is not one continuous concentric layer, but rather built up by at least two different cell populations whose characteristics depend on their position relative to the vasculature.

Lateral root formation is regulated by a complex interplay of different plant hormones (reviewed in Nibau *et al.* [8]). The role of auxin in the whole process has been well characterized in *Arabidopsis* during past decades. Auxin is involved in the specification of founder cells [9], during lateral root organogenesis [10,11] and emergence of the primordium [12]. An oscillating auxin signalling maximum in the protoxylem at the level of the basal meristem specifies the neighbouring pericycle founder cells, and therefore determines the place of lateral root initiation [13–15]. Under controlled growth conditions, lateral root initiation occurs strictly acropetally and alternates

* Author for correspondence (tom.beeckman@psb.vib-ugent.be).

Electronic supplementary material is available at http://dx.doi.org/10.1098/rstb.2011.0239 or via http://rstb.royalsocietypublishing.org.

One contribution of 18 to a Theme Issue 'Root growth and branching'.

between the two xylem poles [14,16]. Whether it is auxin itself that triggers founder cell specification or another signalling molecule, is not yet known. As most work has been focused on *Arabidopsis*, little or no information is available for other plants, including important monocotyledonous crops.

The anatomy of the maize root is more complex than that of the *Arabidopsis* root, with multiple cortex layers and varying numbers of cells per layer. Furthermore, the maize root has an extensive poly-arch vasculature containing on average six to 10 central late meta-xylem elements with two or three xylem poles each, consisting of proto- and early meta-xylem [17,18]. An equal number of phloem poles can be found, which alternate with the xylem tissues in the vascular bundle. Similar to *Arabidopsis*, the vasculature is surrounded by a single layer of pericycle cells from which lateral roots are formed. However, in contrast to *Arabidopsis*, also the endodermis cells take part in the formation of a lateral root primordium in maize [19]. Reports on the exact location of lateral root initiation have been contradictory: Bell & McCully [19] stated that laterals are formed at the xylem poles, as in *Arabidopsis*, while Casero *et al.* [20] found them to initiate in the phloem-pole pericycle cells. The initiation of lateral roots in maize is not strictly acropetal as in *Arabidopsis*, and no regularity was found in the sequence of initiation between the different vascular poles [21]. Detailed characterization of the maize *rum1* mutant, lacking embryonic seminal roots and lateral roots on the primary root, led to the conclusion that most likely auxin accumulation in the pericycle precedes, and is required for, the degradation of RUM1, a maize Aux/IAA repressor protein [22,23]. Furthermore, auxin availability might also be controlled by RUM1 because *rum1* mutants displayed reduced polar auxin transport. In any case, the *rum1* mutant clearly demonstrates the importance of auxin distribution in maize lateral root initiation. However, up to now, information on the localization of auxin in maize roots could only be derived from chromatography and mass spectrometry data [24–26]. These methods detected high levels of auxin in the stele, but detailed spatial information is lacking. Precise localization of auxin in the root could help our understanding of a role for auxin in the determination of lateral root founder cells in maize.

Here, we first confirmed the position of lateral root formation in maize relative to the vascular elements. Further, we looked into the characteristics of the pericycle cell layer and early vascular development. Finally, we analysed auxin response in the maize root and demonstrated a role for localized auxin response maxima in lateral root formation.

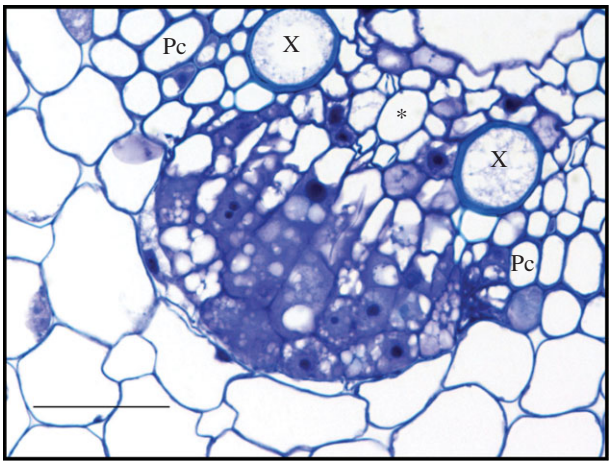

Figure 1. Lateral root formation in maize. Transversal section through a developing lateral root primordium, visualized with Feulgen stain and toluidine blue dye. Pc, pericycle; X, xylem; asterisk, phloem. Scale bar, 50 μm.

2. RESULTS AND DISCUSSION

(a) *Lateral roots are initiated by anticlinal divisions of pericycle cells between the xylem poles*

To determine the site and the division pattern of the very first cell divisions of lateral root formation in maize, 3-day old primary roots were screened for cytokinesis events. Cortex and epidermis tissues were removed to monitor mitotic figures in the pericycle, visualized by Feulgen DNA staining. Under our growth conditions, the first divisions were found on average at 11.9 ± 2 mm from the root tip.

In longitudinal sections from fragments between 10 and 15 mm from the root tip, occasionally nuclei from two adjacent pericycle cells were found to be displaced to their common cell wall (electronic supplementary material, figure S1*a*), leading to asymmetric and anticlinal divisions (electronic supplementary material, figure S1*b*). Periclinal divisions, visualized on transversal sections, result in the formation of a second layer (electronic supplementary material, figure S1*c*). At this stage, divisions in the endodermis could also be observed (electronic supplementary material, figure S1*d*). Both epi-fluorescence and bright field microscopy of sections showed that lateral roots were exclusively formed in front of phloem poles (electronic supplementary material, figure S1*e*,*f*). Despite the initiation of lateral roots at the phloem poles, pericycle cells in the vicinity of both flanking xylem poles also divide at later stages and take part in the formation of the primordium (figure 1).

Our observations thereby confirm that in maize phloem-pole pericycle cells are competent for lateral root initiation, as was earlier described by Casero *et al.* [20]. Although pericycle cells at the xylem poles do not remain quiescent and are later recruited in the developing primordium, they seem not to be competent for lateral root initiation, suggesting these cells are, upon their formation, differentially specified when compared with phloem-pole pericycle cells. Alternatively, a later positional signalling, acting at the phloem poles, might be involved to trigger lateral root initiation.

(b) *Pericycle cell size is linked with vascular development*

In order to detect early differential specification of the pericycle at the xylem poles when compared with the phloem poles, and in the absence of reporter lines for cell identity, a histological approach was followed by making serial cross sections through the root tip,

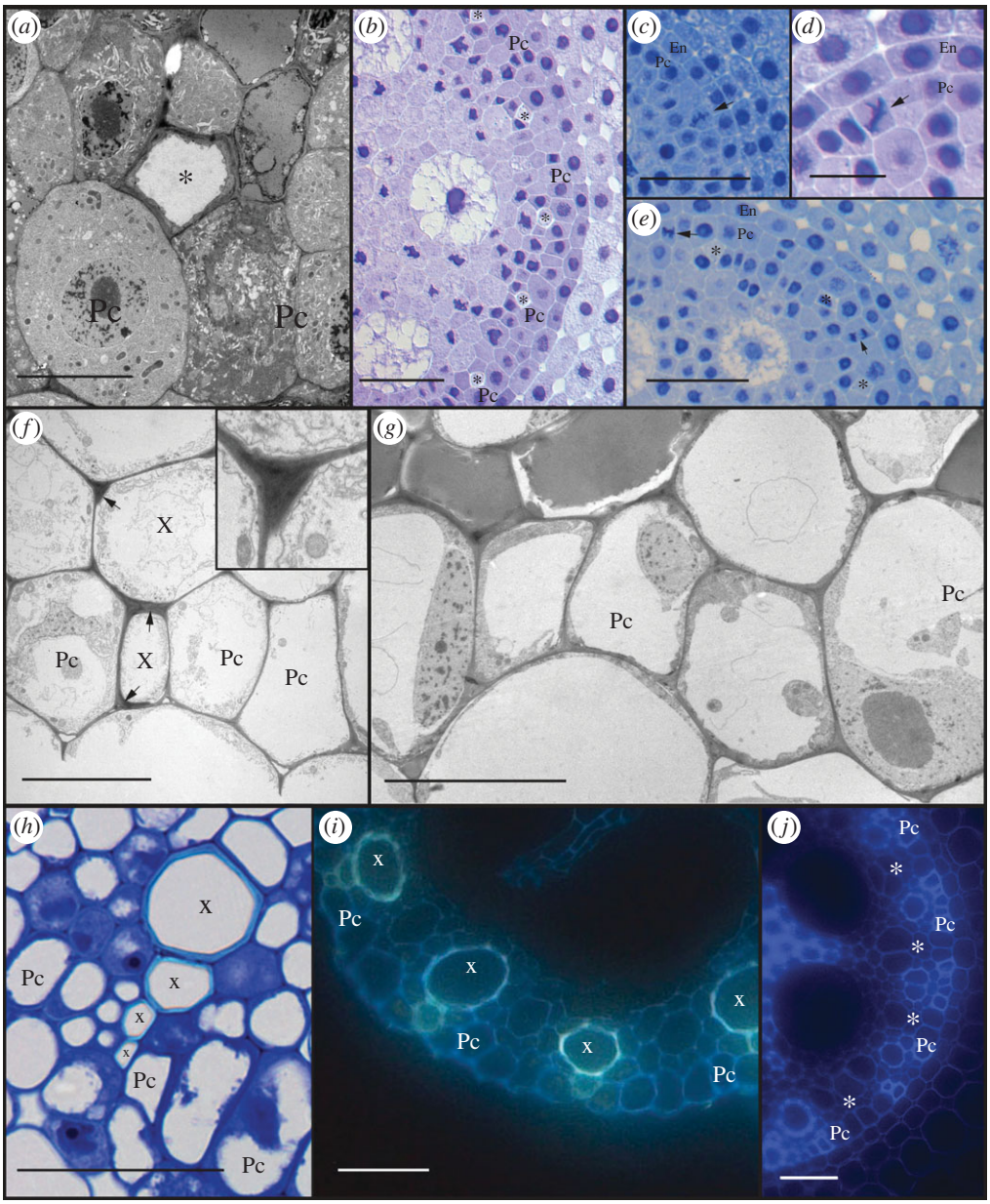

Figure 2. Heterogeneity of the pericycle. (*a*) Transmission electron microscopy (TEM) image through the meristem showing proto-phloem differentiation. (*b*) Light microscopic (LM) image from a section at 900 µm from the root tip where all proto-phloem poles can be recognized. (*c–e*) LM images from sections between 400 and 700 µm from the root tip, showing radial and periclinal divisions (arrowheads) in pericycle cells between the phloem poles. (*f*) TEM image at 10 mm from the root tip showing lignin deposition in xylem cells (arrows). Inset shows detail at higher magnification. (*g*) TEM image of the pericycle at 5 mm from the tip. (*h*) LM image of proto- and early meta-xylem cells (bright blue cell wall) interrupting the pericycle layer. (*i*) Auto-fluorescence of xylem (blue-green) indicates interruption of the pericycle. (*j*) Auto-fluorescence at 35 mm from the tip shows pericycle cells with thick auto-fluorescent cell walls at the xylem poles and thin walls at phloem poles. Roots for LM observations were Feulgen stained and sections were treated with (*b–e*) methylene blue (*h*) or toluidine blue dye. Pc, pericycle; asterisk, phloem; X, xylem. Scale bars: (*a*,*f*,*g*) 10 µm; (*d*) 20 µm; (*b*,*c*,*e*,*h*) 50 µm; (*i*,*j*) 100 µm.

including the root cap and apical meristem. The pericycle cell layer could be observed starting from 350 µm from the tip (including the root cap), while a first sign of vascular differentiation was found at about 700 µm, where diamond-shaped cells of proto-phloem became recognizable by their reduced staining of the cytoplasm and thick nacreous cell walls [27]. Transmission electron microscopy (TEM) on a section through the meristem showed a differentiating proto-phloem sieve element surrounded by meristematic cells (figure 2*a*), indicating the proto-phloem matures prior to all other cell types. At 900 µm from the root tip, all proto-phloem poles could be distinguished (figure 2*b*). Next, cross-sectional surface areas of all pericycle cells were measured, respectively, at 900 µm and at 400 µm distance from the tip. At 900 µm, the average surface area of the two pericycle cells in contact with the proto-phloem element was significantly larger ($185 \pm 33\ \mu m^2$) than the size of other pericycle cells ($112 \pm 35\ \mu m^2$, Student *t*-test, *p*-value < 0.001, electronic supplementary material, figure S2). This implies that, as in *Arabidopsis*, cells prone to lateral root initiation have larger diameters than the other pericycle cells, despite their different position in relation to the

vasculature [28]. In younger tissue, at 400 μm from the root tip, no differences in the surface area between cells at the future phloem poles (70 ± 21 μm^2) and the other pericycle cells (68 ± 24 μm^2, electronic supplementary material, figure S2) could be found. Although we do not have quantitative measurements on the cell division rate in individual pericycle cells, the difference in cell size does not seem to be due to an earlier cell cycle exit of pericycle cells at the phloem poles. Instead, in sections between 400 and 900 μm radial and periclinal divisions were observed in pericycle cells between the phloem poles (figure 2*c–e*), which seem to be at least partially responsible for the smaller cell size found at these sites. While at the phloem poles merely proliferative anticlinal divisions could be seen, the periclinal divisions of pericycle cells between the phloem poles might have a more formative character, in which one or both daughter cells could take part in the formation of the vascular tissues.

The differentiation of xylem vessels can be recognized by the formation of a thick, lignified, cell wall, and in serial sections up to 1 mm, no sign yet of xylem differentiation could be retrieved. Using TEM, signs of lignin deposition were found in sections between 5 and 10 mm from the root tip (figure 2*f*), indicating that proto-xylem formation occurs much later than phloem differentiation, in more differentiated parts of the root. At this level, most pericycle cells had one large central vacuole, characteristic of a differentiated status (figure 2*g*). Intriguingly, at the level of the xylem poles, pericycle cells seemed also to become lignified and recruited into the proto-xylem tissue (figure 2*f*). In about 75 per cent of the analysed xylem poles, the pericycle was interrupted by the proto-xylem (figure 2*h*,*i*). This has also been described earlier for rice [29], but to our knowledge does not occur in *Arabidopsis*.

Apart for the difference in cell size and the interruption of the pericycle by the proto-xylem, variations were found in cell wall thickness. Epi-fluorescence microscopy of unstained vibratome sections revealed smaller xylem-pole pericycle cells with thick, auto-fluorescent cell walls, while the large pericycle cells at the phloem poles had thinner cell walls and lacked auto-fluorescence (figure 2*j*). This further corroborates the heterogeneous character of the pericycle in maize, which is at least partially associated with the maturation of the vasculature.

(c) *Auxin response in the maize root is mainly localized in vascular tissues*

Auxin plays an important role in plant development and lateral root formation. However, no detailed information is available on auxin responses in the maize root. A maize marker line expressing *RFP* (red fluorescent protein) under control of a DR5 auxin responsive promoter [30,31] was used to analyse the spatial characteristics of auxin response in the primary root. This marker line reports the sites where strong degradation activity of the inhibitory Aux/IAA proteins occurs and can thus be regarded as an auxin response maximum marker, but cannot be used to monitor actual auxin concentrations in the tissue.

Longitudinal sections through the root tip revealed auxin response maxima in the root cap, epidermis and vascular tissues (figure 3*a*). On transverse sections, starting at the root tip, RFP signal was first observed in the large meta-xylem precursor cells (figure 3*b*) and in the proto-xylem poles (figure 3*c*). Because auxin is involved in the differentiation of xylem elements [32,33], these auxin response maxima are most probably linked to this differentiation process. About 300–400 μm higher, fluorescent signal was also observed in cells at the phloem poles, in addition to the auxin response maxima at the xylem poles (figure 3*d*). Closer inspection of these sections revealed auxin response maxima in cells surrounding the protophloem elements, possibly companion cells, but not in the pericycle cells (figure 3*d*, inset). At around 5 mm from the root tip, only the RFP signal at the level of the phloem poles remained (figure 3*e*). Although a role for these auxin response maxima in differentiation cannot be excluded, this seems unlikely, as the signal is localized in the surrounding cells and remains in more mature parts of the root. As the auxin response maximum corresponds to the place where lateral roots are formed, it might have a role in the competence of these cells for lateral root initiation, in analogy with the oscillating auxin response maxima in *Arabidopsis* [14,15]. Unfortunately, our method does not allow us to detect variable intensities over time or in specific zones.

Between 10 and 15 mm from the root tip, fluorescence was found in a young lateral root primordium (figure 3*f*). During further development of the lateral root, auxin response maxima were formed at the tip of the primordia (figure 3*g*). Also in the parent root at the level of the stele, where the vascular connection with the lateral root is established, a strong auxin response was detected, particularly at the xylem poles (figure 3*h*), pointing to a role for auxin in the formation of a vascular connection between the lateral and the parent root.

The specific distribution of the auxin response maxima argues for a role of auxin in xylem differentiation, lateral root positioning and lateral root initiation and development in maize.

(d) *Inhibition of auxin transport prevents lateral root initiation and perturbs the formation of auxin response maxima*

In several plants, such as *Arabidopsis* and rice, treatment with 1-*N*-naphthylphthalamic acid (NPA), an auxin transport inhibitor, prevents the formation of lateral roots [34,35]. Further, it was shown that the recurrent auxin response maxima in the protoxylem in *Arabidopsis* do not occur in the presence of NPA [11]. To study the effect of impediment of auxin transport on the formation of lateral roots and the localization of the auxin response maxima in maize, plants were grown in the presence of NPA. In 7-day-old NPA-treated seedlings, no emerged lateral roots could be found (electronic supplementary material, figure S3). In DR5::RFP plants germinated and grown in NPA for 3 days, the clear auxin response maxima present in the vasculature of control roots (figure 3*a*) were not found (figure 4*a*). Instead, a diffuse signal was observed in the stele and

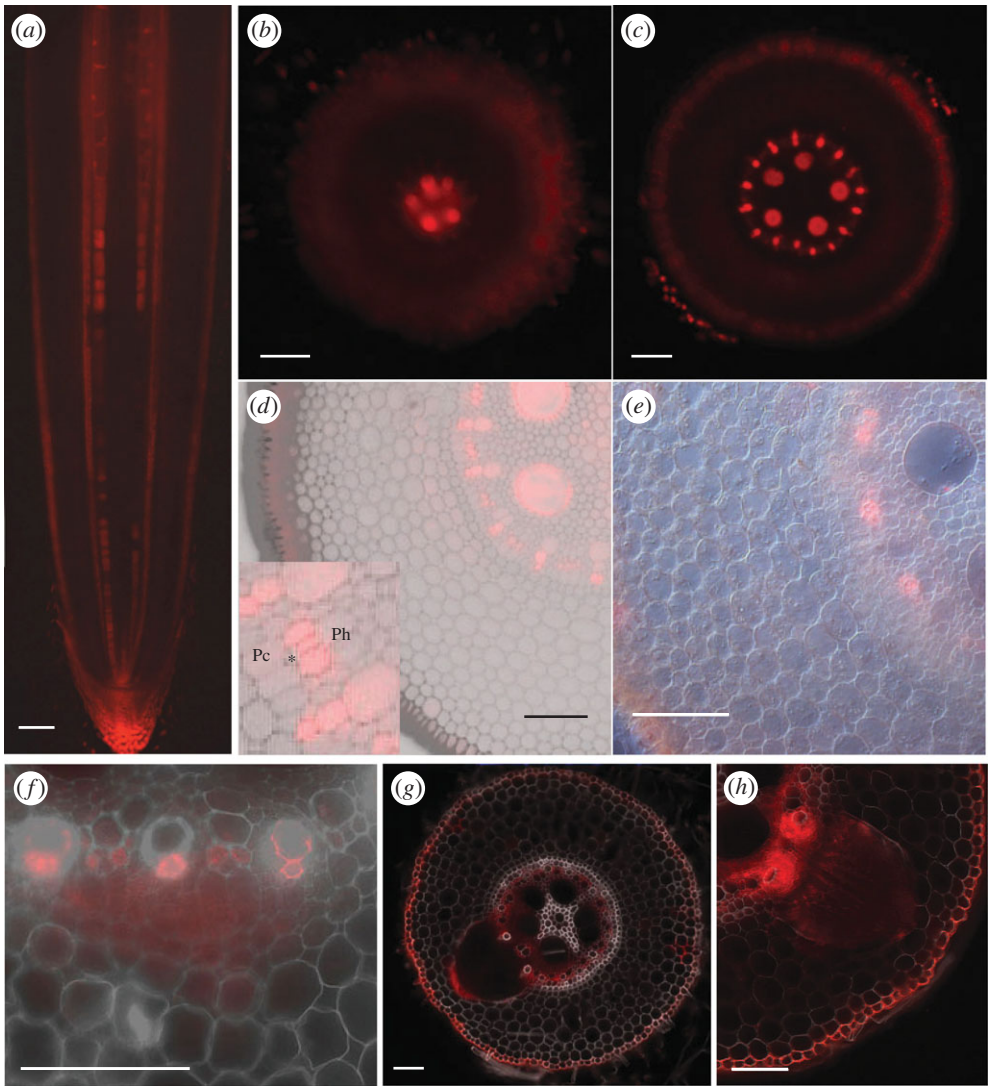

Figure 3. Auxin response in the maize root visualized by DR5::RFP. (*a*) Longitudinal section through the root tip. (*b–e*) Subsequent transverse sections through the apical 5 mm of the root tip. (*b*) Signal appears first in the precursors of the late meta-xylem. (*d*) Signal appears in the proto- and early meta-xylem. (*d*) An auxin response maximum is formed at the phloem poles. Inset shows that RFP is visible in the cells between the proto-phloem (*) and the (future) phloem (Ph). No signal in the pericycle (Pc). (*e*) At 5 mm from the tip, signal at the phloem poles still remains. (*f–h*) Auxin response during lateral root formation. (*f*) In early stages, signal is found in dividing pericycle and endodermis cells. (*g*) An auxin response maximum is formed at the tip of the growing primordium. (*h*) Auxin response maxima at the level of vascular connection with the parent root. Scale bars: (*a*,*e*) 200 μm; (*b–d*, *f–h*) 100 μm.

in cortex tissues, indicating NPA treatment disrupts the normal auxin distribution and/or response in the root. On transverse sections, a fluorescence maximum was still found in the precursors of the meta-xylem; however, the fluorescence was less clear in the rest of the xylem (figure 4*b*). A more diffuse signal was spread over the stele and the inner layers of the cortex, and no auxin response maximum was formed at the level of the phloem poles. In older parts of the root, where in normal conditions the fluorescence signal remained at the phloem poles (figure 3*e*), RFP signal was more diffusely distributed over the whole stele without clear maxima (figure 4*c*).

Despite the disturbed auxin response maxima, the differentiation of the proto-phloem seemed not to be affected at the cellular level, but was even completed closer to the root tip than in control plants (electronic supplementary material, figure S3). This effect might be attributed to the slower growth rate of NPA-grown plants [36], which implies that cells at a similar distance from the root tip are older and thus more differentiated in NPA-treated roots. Nevertheless, even at 5 and 10 mm from the tip, pericycle cells were found with a large central nucleus, surrounded by cytoplasm (figure 4*d*), and numerous smaller vacuoles (figure 4*e*), both characteristic of meristematic cells. This suggests that the NPA treatment keeps pericycle cells in an undifferentiated or cell division competent state.

The effect of long-term NPA treatments on pericycle cell division was evaluated in sections from roots grown in NPA for 5 days. In several roots, zones with ectopic divisions in pericycle and endodermis cells were observed, resulting in multi-layered structures, both at the xylem and phloem poles (figure 4*f–h*). However, no organized lateral root primordia were formed. This phenotype shows strong similarity to auxin-treated

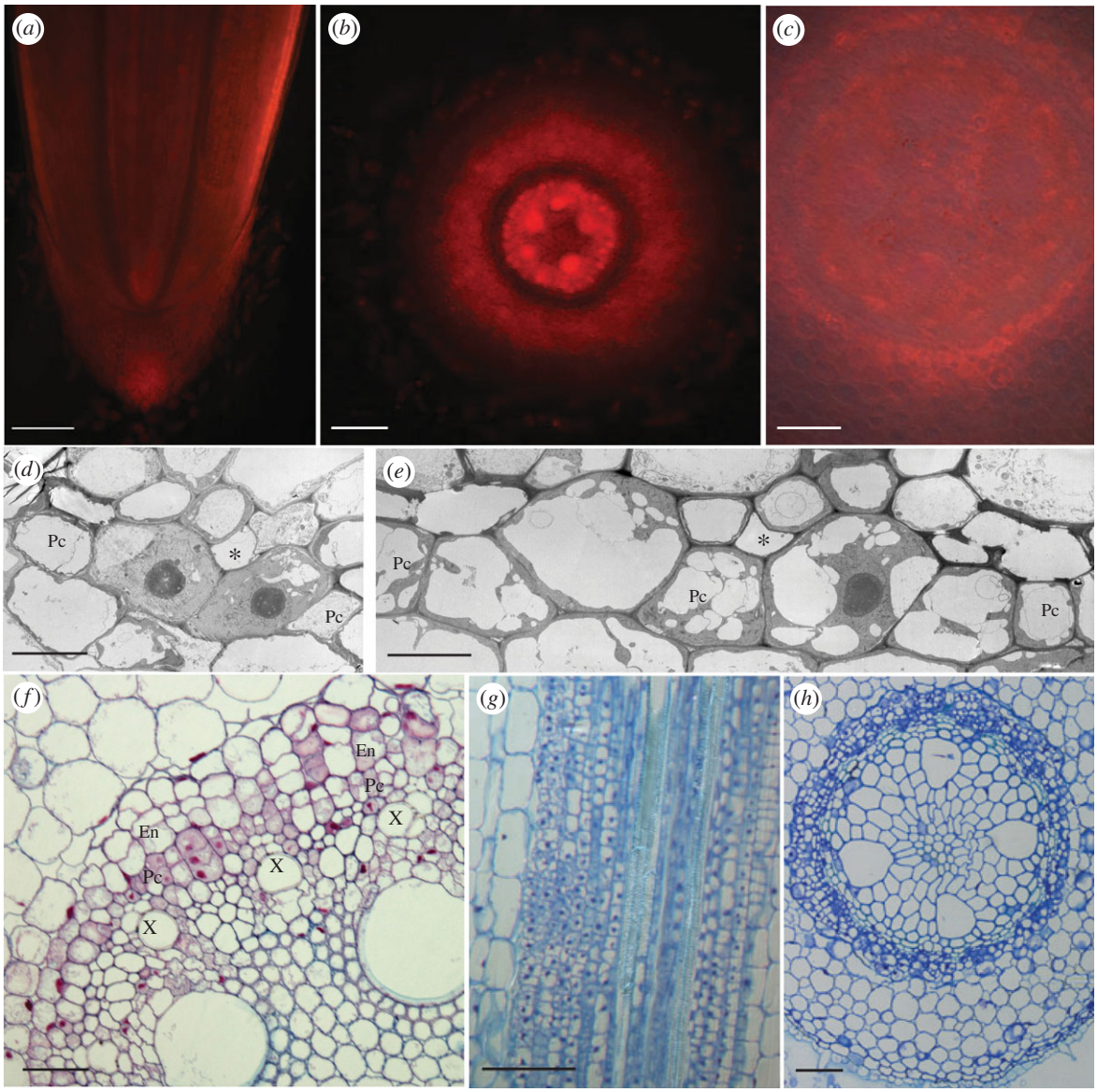

Figure 4. Effect of NPA treatment on auxin response and pericycle differentiation. (*a–c*) Auxin response in roots grown in NPA. (*a*) Longitudinal section through the root tip. (*b*) Despite a diffuse signal spread over the stele and inner cortex, auxin response maxima are found in xylem cells. (*c*) No clear auxin response maxima are formed at the phloem poles. (*d–e*) TEM images of the pericycle. (*d*) Large central nuclei at 5 mm from the tip, and (*e*) several smaller vacuoles at 10 mm from the tip, indicating the pericycle is not fully differentiated. (*f–h*) Ectopic divisions lead to multi-layered pericycle and endodermis. Roots were Feulgen stained, and (*f*) sections were treated with ruthenium red or (*g*,*h*) toluidine blue dye. Pc, pericycle; asterisk, phloem; X, xylem. Scale bars: (*a*) 200 μm; (*b*,*c*,*f*,*g*) 100 μm; (*h*) 50 μm; (*d*,*e*) 10 μm.

roots of the weak alleles of *gnom*^{R5}, an *Arabidopsis* mutant with disturbed cell polarity. Although this mutant does not form lateral roots in control conditions, treatment with the synthetic auxin variants 1-naphthaleneacetic acid (NAA) or 2,4-dichlorophenoxyacetic acid (2,4D) leads to random pericycle cell proliferation [37]. This phenotype is the consequence of a disrupted localization of the PIN1 auxin export protein, hampering the formation of the auxin gradient needed for lateral root initiation and development [37,38]. In maize, the endogenous auxin concentrations might be sufficient to induce cell division, while NPA treatment prevents the formation of localized auxin response maxima and leads to ectopic, proliferative divisions. Transfer of 5-day old NPA-grown plants to NAA, resulted in the formation of lateral roots at nearly every phloem pole (electronic supplementary material, figure S4).

3. CONCLUSIONS

A comparable vascular build-up of auxin response maxima is crucial for lateral root formation in both monocots and dicots, and hints to the existence of evolutionary conserved cell-to-cell communication systems between the vasculature and neighbouring cell layers. Our results further show that, in parallel with *Arabidopsis*, non-polarized auxin distribution may result in non-formative divisions and that orchestrated auxin distribution patterns are required to induce formative cell divisions in maize (figure 5).

4. MATERIAL AND METHODS

(a) *Plant growth*

Analysis of auxin response was performed with a DR5::RFP line (http://maize.jcvi.org/cgi-bin/maize/

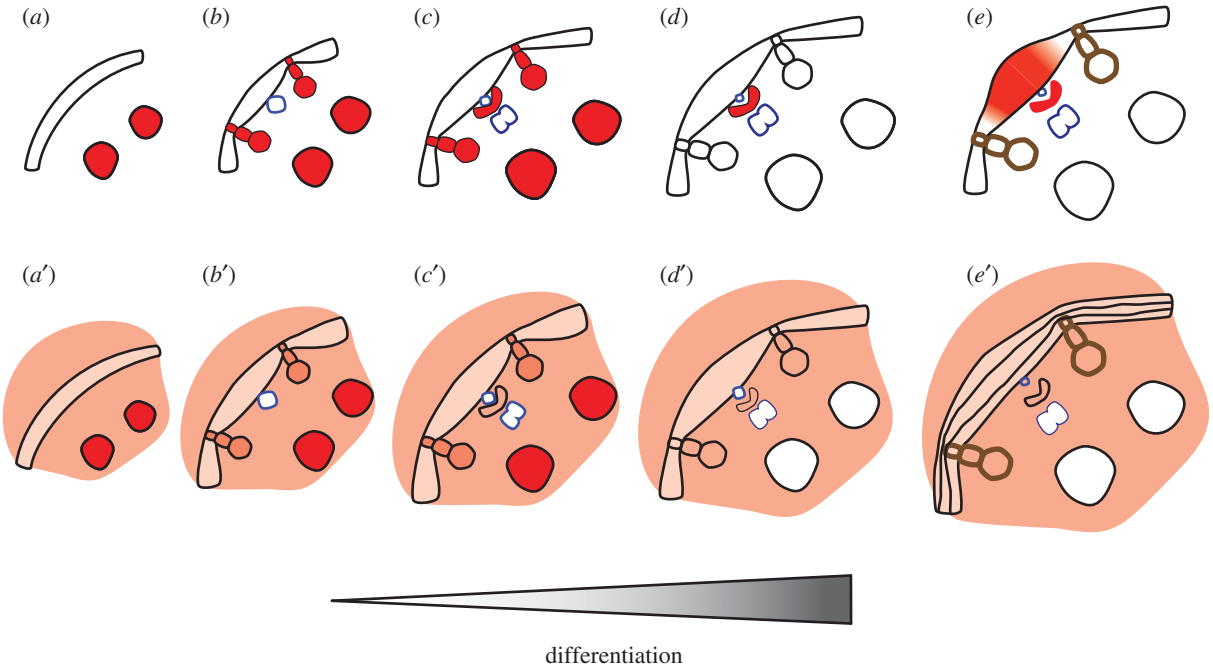

Figure 5. Schematic of the main conclusions. (*a*) Prior to vascular differentiation, the pericycle forms a homogeneous cell layer, and a strong auxin response maximum is present in the large precursors of the late meta-xylem. (*a*′) This auxin response maximum is also formed during NPA treatment, despite a diffuse auxin response spread over the stele. (*b*) Together with the maturation of the proto-phloem, a difference in cell size becomes apparent between cells in contact with the proto-phloem and other pericycle cells. Auxin accumulates in the precursors of proto-xylem and early meta-xylem. (*b*′) NPA treatment has no obvious effect on the auxin response maxima at the xylem poles. (*c*) In the cells surrounding the protophloem, an auxin response maximum is formed. (*c*′) NPA treatment prevents the formation of an auxin response maximum at the phloem poles. (*d*) Lignification of proto-xylem cell walls, the pericycle layer is interrupted by the xylem. Only the auxin response maximum at the phloem poles remains. (*d*′) No auxin response maxima are formed in NPA-treated roots. (*e*) Lateral roots are initiated from pericycle cells between the xylem poles. During lateral root formation, an auxin gradient is formed with a maximum at the tip of the primordium. (*e*′) NPA prevents the formation of lateral roots. No auxin response maxima are formed, and random divisions take place in pericycle and endodermis, resulting in multi-layered structures.

cellgenomics/geneDB_list.pl); for other experiments B73 *Zea mays* inbred line was used. Kernels were surface sterilized in 6 per cent NaOCl for 5 min and rinsed three times with water. Germination and growth took place in water using a paper roll system described before [23] in continuous light at 27°C. For NPA treatment, plants were grown in 50 µM NPA (Duchefa). For NAA treatment, plants were transferred to 50 µM NAA (Sigma-Aldrich). Unless stated differently, analyses were performed on 3-day old seedlings.

(b) *Histology and histochemistry*

(i) *Feulgen staining*

Roots were fixed overnight at 4°C in 4 per cent paraformaldehyde and 1 per cent glutaraldehyde, in phosphate buffer, and rinsed in water. After a 10 min maceration in 1 N HCl at 60°C, roots were rinsed in water and stained with Schiff's Fuchsin–sulphite reagent (Sigma-Aldrich) for about 30 min. After staining, material was incubated three times for 10 min in $K_2S_2O_5$ solution (5 ml 1 N HCl, 5 ml 10 per cent $K_2S_2O_5$, 100 ml H_2O) and rinsed with water.

(ii) *Observation of mitotic figures*

Roots were fixed overnight in a mixture of ethanol and acetic acid (3 : 1). After Feulgen staining, cortex and epidermis tissues were removed from the stele [24]. Roots were mounted in 50 per cent glycerol and observed with a Zeiss Axio-Vert135M epi-fluorescence microscope equipped with a MAC 5000 controller system including a MAC2 XY motor stage controller and a Z-axis/focus controller (Ludl Electronic Products Ltd.). A filter set for rhodamine was used (excitation 546/12 nm; beamsplitter 580 nm; emission 590 nm). The observation was performed on 13 roots.

(iii) *Sectioning*

After fixation and Feulgen staining, root fragments of 5 mm were dehydrated and infiltrated with Technovit 7100 (Heraus Kulzer) as described by Beeckman & Viane [39]. A first embedding step was done in small $6 \times 3 \times 4\ mm^3$ moulds. For longitudinal sections, the method of Beeckman & Viane [39] was used; transverse sections were made as described by De Smet *et al.* [40], using an ultramicrotome (Reichert-Jung Supercut 2050, Germany). Sections were stained with 0.01 per cent toluidine blue, 0.1 per cent methylene blue or 0.05 per cent ruthenium red and mounted with DePeX (Gurr, BDH Chemicals Ltd). Observations were made with an Olympus DX51 in combination with a Nikon DS-Fi1 camera. Cell surface was measured with ImageJ software (http://rsbweb.nih.gov).

(iv) *Localization of auxin response*

Roots were fixed in 4 per cent para-formaldehyde in phosphate buffer for at least 1 h at 4°C. Root fragments of 5 mm were embedded in 6 per cent agarose

with 0.5 per cent gelatine and sections of 100 μm were cut with a vibratome, mounted with distilled water and immediately observed with a Zeiss Axio-Imager epi-fluorescence microscope. A filter set for rhodamine was used (excitation 546/12 nm; beamsplitter 560 nm; emission 575/64 nm). Images were taken with an AxioCam (Zeiss).

(v) *Auto-fluorescence*

Auto-fluorescence was detected on vibratome sections observed with a Zeiss Axio-Imager and images taken with an AxioCam (Zeiss). Two filter sets were used: CFP/YFP (excitation 427/14 and 504/17 nm; beamsplitters 440 and 520 nm; emission 464/32 and 547/43 nm, figure 2*f*) and DAPI (excitation 470/40 nm; beamsplitter 495 nm; emission 525/50 nm; figure 2*h*).

(vi) *Transmission electron microscopy*

For TEM, two different fixation methods were used. For high-pressure freezing (figure 2*a*,*e*), root segments were taken at the meristem and at 5 mm from the tip, and briefly immersed in 20 per cent (w/v) BSA and frozen immediately in a high-pressure freezer (EM Pact, Leica Microsystems, Vienna, Austria). Freeze-substitution was carried out using a Leica EM AFS in dry acetone containing 0.1 per cent uranylcetate, 1 per cent (w/v) OsO_4 and 0.2 per cent glutaraldehyde over a 4-day period as follows: −90°C for 26 h, 2°C per hour increase for 15 h, −60°C for 8 h, 2°C per hour increase for 15 h and −30°C for 8 h. Samples were then slowly warmed up to 4°C, infiltrated stepwise over 3 days at 4°C in Spurr's resin and embedded in capsules. The polymerization was performed at 70°C for 16 h. For chemical fixation (figures 2*d* and 4*d*,*e*), root fragments taken at 5 and 10 mm from the tip were excised on 0.5 and 1 cm and immersed in a fixative solution of 2.5 per cent glutaraldehyde and 4 per cent formaldehyde in Na-cacodylate buffer 0.1 M with $CaCl_2$ (20 mg per 100 ml), placed in a vacuum oven for 30 min and left rotating for 3 h at room temperature. This solution was later replaced with fresh fixative and samples were left rotating over night at 4°C. After washing, samples were post fixed in 1 per cent OsO_4 with $K_3Fe(CN)_6$ in 0.1 M Na-cacodylate buffer, pH 7.2. Samples were dehydrated through a graded ethanol series, including a bulk staining with 2 per cent uranyl acetate at the 50 per cent ethanol step followed by embedding in Spurr's resin. Ultrathin sections were made using an ultramicrotome (Leica EM UC6) and post-stained in a Leica EM AC20 for 40 min in uranyl acetate at 20°C and for 10 min in lead stain at 20°C. Grids were viewed with a JEM 1010 transmission electron microscope (JEOL, Tokyo, Japan) operating at 80 kV.

(vii) *Treatment of the images*

For all methods, pictures were processed with Photoshop CS4.

We thank Dr Boris Parizot and Dr Giel van Noorden for critical reading and suggestions. We are grateful to Dr Daniel Van Damme for the use of the MAC5000 controller system, financially supported by an FWO Research Grant (grant number 1.5.232.08.N.00). This work was supported by grants from the Interuniversity Attraction Poles Programme (IUAP VI/33), initiated by the Belgian State, Science Policy Office.

REFERENCES

1 Dolan, L., Janmaat, K., Willemsen, V., Linstead, P., Poethig, S., Roberts, K. & Scheres, S. 1993 Cellular organisation of the *Arabidopsis thaliana* root. *Development* **119**, 71–84.
2 Ito, K., Tanakamaru, K., Morita, S., Abe, J. & Inanaga, S. 2006 Lateral root development, including responses to soil drying, of maize (*Zea mays*) and wheat (*Triticum aestivum*) seminal roots. *Physiol. Plantarum* **127**, 260–267. (doi:10.1111/j.1399-3054.2006.00657.x)
3 Varney, G. T. & Canny, M. J. 1993 Rates of water uptake into the mature root system of maize plants. *New Phytol.* **123**, 775–786. (doi:10.1111/j.1469-8137.1993.tb03789.x)
4 Dubrovsky, J. G., Doerner, P. W., Colon-Carmona, A. & Rost, T. L. 2000 Pericycle cell proliferation and lateral root initiation in *Arabidopsis*. *Plant Physiol.* **124**, 1648–1657. (doi:10.1104/pp.124.4.1648)
5 Parizot, B. *et al.* 2008 Diarch symmetry of the vascular bundle in *Arabidopsis* root encompasses the pericycle and is reflected in distich lateral root initiation. *Plant Physiol.* **146**, 140–148. (doi:10.1104/pp.107.107870)
6 De Smet, I., Vanneste, S., Inze, D. & Beeckman, T. 2006 Lateral root initiation or the birth of a new meristem. *Plant Mol. Biol.* **60**, 871–887. (doi:10.1007/s11103-005-4547-2)
7 Parizot, B., De Rybel, B. & Beeckman, T. 2010 VisuaLRTC: a new view on lateral root initiation by combining specific transcriptome data sets. *Plant Physiol.* **153**, 34–40. (doi:10.1104/pp.109.148676)
8 Nibau, C., Gibbs, D. J. & Coates, J. C. 2008 Branching out in new directions: the control of root architecture by lateral root formation. *New Phytol.* **179**, 595–614. (doi:10.1111/j.1469-8137.2008.02472.x)
9 Dubrovsky, J. G., Sauer, M., Napsucialy-Mendivil, S., Ivanchenko, M. G., Friml, J., Shishkova, S., Celenza, J. & Benkova, E. 2008 Auxin acts as a local morphogenetic trigger to specify lateral root founder cells. *Proc. Natl Acad. Sci. USA* **105**, 8790–8794. (doi:10.1073/pnas.0712307105)
10 Benková, E., Michniewicz, M., Sauer, M., Teichmann, T., Seifertová, D., Jürgens, G. & Friml, J. 2003 Local, efflux-dependent auxin gradients as a common module for plant organ formation. *Cell* **115**, 591–602. (doi:10.1016/S0092-8674(03)00924-3)
11 De Smet, I. *et al.* 2010 Bimodular auxin response controls organogenesis in *Arabidopsis*. *Proc. Natl Acad. Sci. USA* **107**, 2705–2710. (doi:10.1073/pnas.0915001107)
12 Swarup, K. *et al.* 2008 The auxin influx carrier LAX3 promotes lateral root emergence. *Nat. Cell Biol.* **10**, 946–954. (doi:10.1038/ncb1754)
13 De Rybel, B. *et al.* 2010 A novel aux/IAA28 signaling cascade activates GATA23-dependent specification of lateral root founder cell identity. *Curr. Biol.* **20**, 1697–1706. (doi:10.1016/j.cub.2010.09.007)
14 De Smet, I. *et al.* 2007 Auxin-dependent regulation of lateral root positioning in the basal meristem of *Arabidopsis*. *Development* **134**, 681–960. (doi:10.1242/dev.02753)
15 Moreno-Risueno, M. A., Van Norman, J. M., Moreno, A., Zhang, J., Ahnert, S. E. & Benfey, P. N. 2010 Oscillating gene expression determines competence for periodic *Arabidopsis* root branching. *Science* **329**, 1306–1311. (doi:10.1126/science.1191937)
16 Dubrovsky, J. G., Gambetta, G. A., Hernández-Barrera, A., Shishkova, S. & González, I. 2006 Lateral root initiation in *Arabidopsis*: developmental window, spatial patterning, density and predictability. *Ann. Bot.* **97**, 903–915. (doi:10.1093/aob/mcj604)

17 Feldman, L. 1994 The maize root. In *The maize handbook* (eds M. Freeling & V. Walbot), pp. 29–37. New York, NY: Springer.
18 Hochholdinger, F. 2009 The maize root system: morphology, anatomy, and genetics. In *The handbook of maize* (eds J. Bennetzen & S. Hake), pp. 145–160. New York, NY: Springer.
19 Bell, J. K. & McCully, M. E. 1970 A histological study of lateral root initiation and development in *Zea mays*. *Protoplasma* **70**, 179–205. (doi:10.1007/BF01276979)
20 Casero, P., Casimiro, I. & Lloret, P. 1995 Lateral root initiation by asymmetrical transverse divisions by pericycle cells in four plant species: *Raphanus sativus*, *Helianthus anuus*, *Zea mays*, and *Daucus carota*. *Protoplasma* **188**, 49–58. (doi:10.1007/BF01276795)
21 MacLeod, R. D. 1990 Lateral root primordium inception in *Zea mays*. *Environ. Exp. Bot.* **30**, 225–234. (doi:10.1016/0098-8472(90)90068-F)
22 von Behrens, I., Komatsu, M., Zhang, Y., Berendzen, K. W., Niu, X., Sakai, H., Taramino, G. & Hochholdinger, F. 2011 Rootless with undetectable meristem 1 encodes a monocot-specific AUX/IAA protein that controls embryonic seminal and post-embryonic lateral root initiation in maize. *Plant J.* **66**, 341–353. (doi:10.1111/j.1365-313X.2011.04495.x)
23 Woll, K., Borsuk, L. A., Stransky, H., Nettleton, D., Schnable, P. S. & Hochholdinger, F. 2005 Isolation, characterization, and pericycle-specific transcriptome analyses of the novel maize lateral and seminal root initiation mutant *rum1*. *Plant Physiol.* **139**, 1255–1267. (doi:10.1104/pp.105.067330)
24 Saleem, M., Lamkemeyer, T., Schutzenmeister, A., Madlung, J., Sakai, H., Piepho, H. P., Nordhiem, A. & Hochholdinger, F. 2010 Specification of cortical parenchyma and stele of maize primary roots by asymmetric levels of auxin, cytokinin, and cytokinin-regulated proteins. *Plant Physiol.* **152**, 4–18. (doi:10.1104/pp.109.150425)
25 Bridges, I. G., Hillman, J. R. & Wilkins, M. B. 1973 Identification and localisation of auxin in primary roots of *Zea mays* by mass spectrometry. *Planta* **115**, 189–192. (doi:10.1007/BF00387784)
26 Greenwood, M. S., Hillman, J. R., Shaw, S. & Wilkins, M. B. 1973 Localization and identification of auxin in roots of *Zea mays*. *Planta* **109**, 369–374. (doi:10.1007/BF00387107)
27 Evert, R. 1977 Phloem structure and histochemistry. *Annu. Rev. Plant Physiol.* **28**, 199–222. (doi:10.1146/annurev.pp.28.060177.001215)
28 Laskowski, M. J., Williams, M. E., Nusbaum, H. C. & Sussex, I. M. 1995 Formation of lateral root meristems is a two-stage process. *Development* **121**, 3303–3310.
29 Kawata, S., Morita, S. & Yamazaki, K. 1978 On the differentiation of vessels and sieve tubes at the root tips of rice plants. *Jpn J. Crop Sci.* **47**, 101–110. (doi:10.1626/jcs.47.101)
30 Mohanty, A. *et al.* 2009 Advancing cell biology and functional genomics in maize using fluorescent protein-tagged lines. *Plant Physiol.* **149**, 601–605. (doi:10.1104/pp.108.130146)
31 Ulmasov, T., Murfett, J., Hagen, G. & Guilfoyle, T. J. 1997 Aux/IAA proteins repress expression of reporter genes containing natural and highly active synthetic auxin response elements. *Plant Cell* **9**, 1963–1971. (doi:10.2307/3870557)
32 Yoshida, S., Iwamoto, K., Demura, T. & Fukuda, H. 2009 Comprehensive analysis of the regulatory roles of auxin in early transdifferentiation into xylem cells. *Plant Mol. Biol.* **70**, 457–469. (doi:10.1007/s11103-009-9485-y)
33 Dettmer, J., Elo, A. & Helariutta, Y. 2009 Hormone interactions during vascular development. *Plant Mol. Biol.* **69**, 347–360. (doi:10.1007/s11103-008-9374-9)
34 Casimiro, I. *et al.* 2001 Auxin transport promotes *Arabidopsis* lateral root initiation. *Plant Cell* **13**, 843–852. (doi:10.2307/3871344)
35 Sreevidya, V. S., Hernandez-Oane, R. J., Gyaneshwar, P., Lara-Flores, M., Kadha, J. K. & Reddy, P. M. 2010 Changes in auxin distribution patterns during lateral root development in rice. *Plant Sci.* **178**, 531–538. (doi:10.1016/j.plantsci.2010.03.004)
36 Rahman, A., Bannigan, A., Sulaman, W., Pechter, P., Blancaflor, E. B. & Baskin, T. I. 2007 Auxin, actin and growth of the *Arabidopsis thaliana* primary root. *Plant J.* **50**, 514–528. (doi:10.1111/j.1365-313X.2007.03068.x)
37 Geldner, N., Richter, S., Vieten, A., Marquardt, S., Torres-Ruiz, R. A., Mayer, U. & Jurgens, G. 2004 Partial loss-of-function alleles reveal a role for GNOM in auxin transport-related, post-embryonic development of *Arabidopsis*. *Development* **131**, 389–400. (doi:10.1242/dev.00926)
38 Geldner, N. *et al.* 2003 The *Arabidopsis* GNOM ARF-GEF mediates endosomal recycling, auxin transport, and auxin-dependent plant growth. *Cell* **112**, 219–230. (doi:10.1016/S0092-8674(03)00003-5)
39 Beeckman, T. & Viane, R. 1999 Embedding thin plant specimens for oriented sectioning. *Biotechnic Histochem.* **75**, 23–26. (doi:10.3109/10520299009047981)
40 De Smet, I., Chaerle, P., Vanneste, S., De Rycke, R., Inze, D. & Beeckman, T. 2004 An easy and versatile embedding method for transverse sections. *J. Microsc.* **213**, 76–80. (doi:10.1111/j.1365-2818.2004.01269.x)